Effect of Desulfonation of Lignosulfonate on the Properties of Poly(Lactic Acid)/Lignin Composites

Hanzhou Ye,[a,b] Yang Zhang,[a,b,*] and Zhiming Yu [a,b,*]

To utilize the lignin generated by the paper industry and reduce the cost of poly(lactic acid) (PLA), PLA/lignin composites were prepared from PLA and different ratios of lignosulfonate (LS) or desulfonated lignosulfonate (DLS) particles using a casting method. The physicochemical properties of the lignins were characterized by Fourier transform infrared spectroscopy (FTIR), thermogravimetric analysis (TGA), differential scanning calorimetry (DSC), gel permeation-high performance liquid chromatography (GPC), and elementary analysis. The results indicate that the sulfur content of the original LS was successfully reduced to half by desulfonation to produce DLS, which was found to have a higher thermal stability and a lower average molecular weight than LS. Additionally, the thermal stability, crystallization, compatibility, mechanical, hydrophobicity, and optical properties of the PLA/lignin composites were also meticulously evaluated. Comparison of the PLA/DLS and PLA/LS composites revealed that the incorporation of DLS into PLA improved compatibility, thermal stability ($T_{5\%}$ and T_{max}), and hydrophobicity, while the mechanical properties remained almost unchanged. In addition, both PLA/DLS and PLA/LS exhibited UV light absorption capacity. Finally, the low-rate addition of both LS (10%) and DLS (5%) accelerated the crystallization of PLA, but crystallization was delayed with higher lignin content.

Keywords: Lignin; Lignosulfonate; Poly(lactic acid); Casting; Desulfonation

Contact information: a: Beijing Key Laboratory of Wood Science and Engineering, Beijing Forestry University, Beijing 100083, China; b: Ministry of Education Key Laboratory of Wooden Material Science and Application, Beijing Forestry University, Beijing 100083, China;
** Corresponding authors: bjfuzhangyang@bjfu.edu.cn; yuzhiming@bjfu.edu.cn*

INTRODUCTION

Lignin is the second most abundant non-food biopolymer on the planet. The chemical structure of lignin is sometimes difficult to define, given that its structure and properties largely depend on the isolation process and the source type used for its extraction (Agrawal *et al.* 2014; Gordobil *et al.* 2014; Thakur and Thakur 2015).

Commercially, lignin is mostly obtained as a by-product of the pulp and paper industry. However, most lignin is consumed as a fuel or energy source, and at present, only approximately 2% of the annually produced lignin is being commercialized (Saito *et al.* 2014). Recent industrial applications of lignin are primarily lignosulfonate (LS)-based materials (Liang *et al.* 2013). Most of the LS is precipitated from spent process liquid and black liquid from sulfite plants by the treatment with lime during the pulping process (Agrawal *et al.* 2014).

Currently, the global production of LS is 1.1 million tons per year, and the market for LS remains restricted and focused on soil stabilizers (Indraratna *et al.* 2012), concrete plasticizers (Surendra *et al.* 2015), cement dispersants (Lummer and Plank 2012), oil well drilling agents (Chen *et al.* 2014a), and adhesive agents (Brizius and Montgomery 2014). In addition, it has also been mixed with certain conventional petroleum-based polymers, such as polyurethane (PU) (Hatakeyama *et al.* 2013; Ferry *et al.* 2015), polypropylene (PP) (Yu *et al.* 2012; Bozsódi *et al.* 2016), polyvinyl alcohol (PVA) (Li 2011; Ye *et al.* 2016), and polyethylene (PE) (Hu and Guo 2015). LS has also been used as an antioxidant to increase the UV resistance of materials (Afrin *et al.* 2012; Yang *et al.* 2015) and as a flame retardant to increase polymer stability (Pan *et al.* 2016), which has enhanced its value and expanded its use.

Admittedly, environmental concerns and a depletion of petroleum resources have driven efforts to prepare bioplastics from renewable materials. Several studies have been carried out on biopolymer/LS composites, with the aim of enhancing the mechanical properties and crystallization (Lin *et al.* 2011; Duval *et al.* 2013) of the biopolymer matrix. Poly(lactic acid) (PLA), a biodegradable and aliphatic polyester material, is derived from plants, such as corn, sugar beets, and wheat. As it has been considered one of the most promising environmentally-friendly, sustainable development polymers (Gordobil *et al.* 2014; Alay *et al.* 2016), PLA is being extensively studied with the aim of replacing commodity polymers. Although PLA is recyclable and compostable with good stiffness and strength, it has its own obvious drawbacks, such as inferior moisture sensitivity, early physical aging, poor impact resistance, and a relatively high price, which limit its extensive use (Imre *et al.* 2013; Liu *et al.* 2016).

LS, used as a natural antioxidant and low-cytotoxicity additive, shows great potential in food packaging (Núñez-Flores *et al.* 2012; Domenek *et al.* 2013) and in the newsprint paper industry (Komissarenkov and Lukanina 2012; Pang *et al.* 2016). Additionally, the inexpensive, renewable lignin is a good candidate to be a filler for PLA composites and also to increase the antioxidant activity of polymers (Zafar *et al.* 2016). However, with the incorporation of a hydrophilic LS filler, the water absorption of the obtained composites inevitably increases (Pye 2008; Revin *et al.* 2016), leading to accelerated biodegradation of the polymer/LS due to the increase of hydrophilicity (Lin *et al.* 2011), which is disadvantageous for PLA/lignin composites. As a strong hydrophilic group, sulfonic acid group plays a key role in the hydrophilicity of LS. Reducing the content of sulfonic acid group in LS can lower the hydrophilicity of the PLA/LS, and thus diminish the biodegradation of composites. The application of desulfonation of LS has been reported in nitrogenous fertilizers (Fischer and Schiene 2002) and oil recovery (DeBons *et al.* 1992). However, to the best of our knowledge, the desulfonation of LS in polymer/LS composites has not been reported yet.

In this study, the number of hydrophilic groups of LS was lowered to produce desulfonated LS (DLS), leading to the enhancement of the hydrophobic qualities of LS. DLS was obtained by the desulfonation of LS, which greatly reduces the sulfonic acid group and thus decreases the water sensibility of the resultant polymer. Byproducts that are released, when lignin is heated, can impair polymer thermal stability (Sallem-Idrissi *et al.* 2016). Thus, the effect of the process of desulfonation of lignosulfonate on the properties of the resultant composites prepared by a casting method were investigated.

EXPERIMENTAL

Materials

PLA 4032D (NatureWorks LLC, Minnetonka, MN, USA), contained less than 2% D-LA with a molecular weight of between 220,000 and 240,000 g mol^{-1}. The glass transition temperature (T_g) and melting point (T_m) of this PLA are 58 °C and 160 °C, respectively. The LS used in this study was supplied by Fuchen Chemical Reagents Factory (Tianjin, China). All other reagents were of analytical grade and used as received.

Desulfonation of LS

A predetermined amount of alkali was added to the LS solution to produce DLS by hydrolysis. Fifty grams of LS and 4 g of NaOH were dissolved in 500 mL of distilled water in a three-necked flask incubated in an oil bath at 180 °C for 3 h. Then, after the solution was cooled to 90 °C, 200 mL of 15% H_2SO_4 were added to the flask and stirred with a magnetic stirrer at ambient temperature for 1.5 h. Subsequently, the product was collected by suction filtration, washed with distilled water, and dried in a vacuum drying chamber at 40 °C until it reached a constant weight.

Composite Preparation

Lignin particles (LS or DLS) were introduced into a PLA matrix to generate PLA/lignin composites by a casting method. Briefly, totally dried PLA (2 g) was dissolved in 20 mL of dichloromethane (DCM) with magnetic stirring at room temperature. Different weight contents of LS or DLS (5%, 10%, or 20%) were added to the PLA solutions obtained above and mixed evenly at room temperature by ultrasonication at 50 Hz for 10 min. The solutions were cast onto a Teflon® mold (200 mm × 200 mm) and dried at room temperature for 24 h. Then, the obtained composites were placed into a vacuum drying chamber at 40 °C for 48 h to totally remove the residual solvent. The resulting dried composites were peeled from the mold, and their thickness were approximately 30 μm. The designated codes of LS, DLS, and the PLA/lignin composites are listed in Table 1.

Table 1. Nomenclature for the Obtained Lignins and PLA/Lignin Composites

Sample Code	PLA loading (%)	LS loading (%)	DLS loading (%)
LS	-	100	-
DLS	-	-	100
PLA	100	-	-
PLA/LS5	95	5	-
PLA/LS10	90	10	-
PLA/LS20	80	20	-
PLA/DLS5	95	-	5
PLA/DLS10	90	-	10
PLA/DLS20	80	-	20

Characterization

Fourier transform infrared (FTIR) spectroscopy analysis

FTIR spectra of the samples were recorded in the spectral range from 600 to 4000 cm^{-1} using a Vertex 70 FTIR spectrophotometer (Bruker, Ettlingen, Germany).

Gel permeation-high performance liquid chromatography (GPC) analysis

The average molecular weight (M_w) and polydispersity (M_w/M_n) of the lignins were studied by gel permeation-high performance liquid chromatography (GPC) using a Waters 1525 system (Waters Corp., Milford, MA, USA). Tetrahydrofuran (THF) eluent was used as the GPC mobile phase, at a flow rate of 1 mL min^{-1} and 35 °C. A Waters 1424 pump index detector and a column PL gel 5 μm mixed-C (Agilent, USA) were employed. Calibration was performed using polystyrene standards.

Elemental analysis

An elemental analyzer (KZDL-8A sulfur auto-analyzer, Tianguan Instrument Co. Ltd., Henan, China) was applied for quantitative analysis of sulfur content in the LS and DLS, using the colorimetric titration method, according to ASTM D3246-15 (2015).

Thermal properties test

The thermal degradation patterns of all the specimens were determined with a Q50 thermogravimetric analyzer (TGA) (TA Instruments, New Castle, DE, USA). The samples were vacuum-dried at 40 °C for 24 h before the test. Approximately 5 to 10 mg of the sample was placed on a platinum cup, and the results were recorded in the range from room temperature up to 600 °C, at a heating rate of 10 °C min^{-1} under a nitrogen atmosphere. The peak temperature at the maximum degradation rate was calculated.

In addition, the glass transition temperature (T_g) of the samples was recorded by differential scanning calorimetry (DSC). Several 3-mg samples were placed in sealed aluminum pans; an empty pan was used as a reference. The samples were first heated to 100 °C and held at this temperature for 5 min, then cooled to 0 °C at a rate of 20 °C min^{-1} for 5 min. Subsequently, the samples were heated at 20 °C min^{-1} to a final temperature of 200 °C (second cycle). The T_g was determined according to the second heating run to avoid the influence of the thermal history.

X-ray diffraction (XRD) analysis

The X-ray diffraction patterns of neat PLA and PLA/lignin composites were determined with an X' Pert PRO MPD X-ray diffractometer (Philips, Amsterdam, the Netherlands), using Cu Kα radiation (λ = 1.5406 Å). Scattered radiation was detected in the range of 2θ from 5° to 55°, at a scan rate of 5° min^{-1}.

Scanning electron microscopy (SEM) analysis

The cross-section (fractured in liquid nitrogen) and the surface morphology of the specimens were examined by SEM. Samples were coated with gold by an auto-fine coater (JFC-1600, JEOL Ltd., Tokyo, Japan) and characterized by field-emission scanning electron microscopy and scanning transmission electron microscopy

(FESEM/STEM) on a JEOL JSM-6700F microscope (JEOL USA Inc., Peabody, MA, USA) operating at 5 kV.

Contact angle

Water contact angle measurements were carried out using a contact angle analyzer (OCA 20 DataPhysics Instruments GmbH, Filderstadt, Germany) with a 3 μL dosing volume and a 1 μL s^{-1} dosing rate. All the specimens were pasted on a slide glass before measurement. Five drops per sample were placed on the surface and measured.

UV−visible spectroscopy (UV−vis)

The transparency of the samples was determined by UV-Vis spectra recorded in the absorbance region from 190 to 400 nm using a TU-1901 spectrophotometer (Beijing Purkinje General Instrument Co., Ltd., Beijing, China), using neat PLA as a reference.

Tensile tests

Samples with the dimension of 80 mm × 10 mm (length and width) were prepared and the tensile strength and Young's modulus were recorded at 24 °C and 25% relative humidity using an INSTRON 3365 universal testing machine (INSTRON, Norwood, MA, USA), with a loading cell of 100 N and a speed of 2 mm min^{-1}. Five replicates per sample were used, and average values are reported.

RESULTS AND DISCUSSION

Properties of LS and DLS

FTIR spectra

A possible schematic of the desulfonation reaction of LS is depicted in Fig. 1. The peak assignments for the infrared absorption bands for LS, DLS, and kraft lignin (KL), are based on the characteristic bands of lignin reported in previous literature (Keshk and Sameshima 2006; Suganuma *et al.* 2008; Lisperguer *et al.* 2009; Yang *et al.* 2014; Kim *et al.* 2015; Shankar *et al.* 2015; Strassberger *et al.* 2015) and are shown in Fig. 2. The spectrum of DLS is similar to that of KL. Aromatic ring bands and the C-H deformation between 1515 and 1460 cm^{-1} are very similar for DLS and KL, but the peaks of LS are ambiguous. The strength and broadening of these peaks were probably associated with the overlap of neighboring peaks at 1591 and 1419 cm^{-1}. However, the overlapping of FTIR absorption bands often makes it difficult to perform direct peak assignments of chemical constituents (Zhou *et al.* 2011).

Compared with LS, the basic structure of lignin remained in the DLS after desulfonation. Bands centered around 2937 and 2850 cm^{-1} can be attributed to C-H stretching vibrations of CH_2, CH_3, and tertiary CH groups in the DLS and KL. Another peak at 1724 cm^{-1} in DLS and KL can be attributed to ester carbonyl vibrations from the feruloyl, acetyl, and *p*-coumaryl groups in lignin.

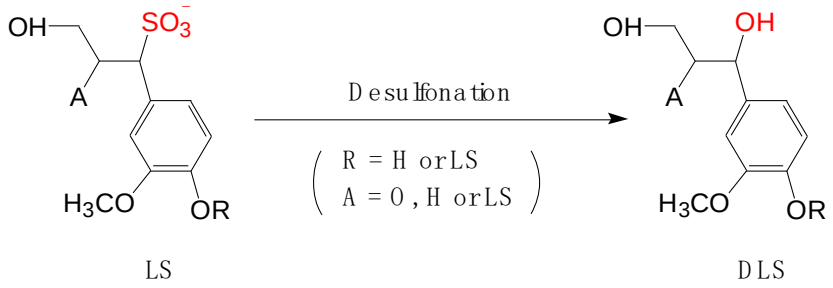

Fig. 1. A possible schematic of the desulfonation reaction of LS

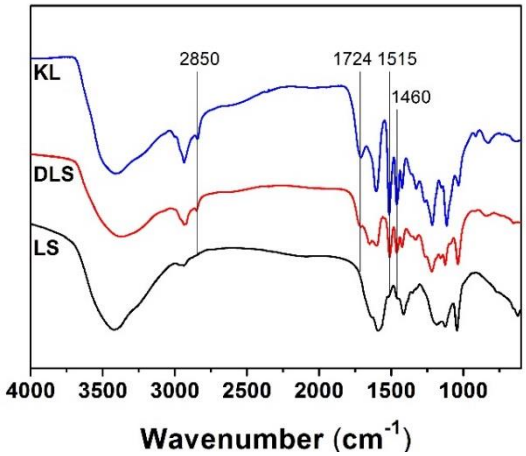

Fig. 2. FTIR spectra of LS and DLS

Molecular weight distribution and sulfur content

The weight averages of lignin differ greatly as a result of the feedstock and the extraction process used (Gordobil *et al.* 2014, 2015). According to the literature, the weight average (M_w) of lignin was detected from 649 to 10680 g·mol^{-1} and the number average (M_n) was from 376 to 4900 g·mol^{-1} (Scholze *et al.* 2001). The values of the M_n, M_w, polydispersity (M_w/M_n), and total sulfur content of both lignins are listed in Table 2. In this case, as the value of the total sulfur content declined after desulfonation, the molecular weight of the DLS was found to decrease due to the rupture of the bonds in LS. Similarly, for both LS and DLS, a narrow molecular weight distribution was indicative of a relatively low value of polydispersity (El Mansouri and Salvadó 2006; El Hage *et al.* 2009). Moreover, in our case, the total sulfur content of DLS was lower than that of LS, indicating that the desulfonation process occurred.

Table 2. Number Average (M_n), Weight Average (M_w), Polydispersity (M_w/M_n), and Total Sulfur Content of LS and DLS

Sample Code	M_n (g·mol^{-1})	M_w (g·mol^{-1})	M_w/M_n	Total Sulfur Content (%)
LS	2317	2329	1.00	5.78 ± 0.58
DLS	604	635	1.05	2.32 ± 0.11

Thermal stability

The thermogravimetric analysis (TGA) was conducted from room temperature up to 600 °C under a nitrogen atmosphere, and the derivative thermogravimetric (DTG) curves of LS and DLS were obtained (Fig. 3). The DTG curves indicated that the degradation of LS was more complex than that of DLS, with some peaks and plateaus throughout the whole range of temperatures. The weight loss of the DLS was associated with two main stages (Li and McDonald 2014). The degradation of LS occurred in three steps, which is consistent with other research (Li *et al.* 2014).

The first stage of the degradation of DLS and LS began at approximately 150 °C, while the second stage of the degradation of DLS was centered at approximately 250 to 400 °C. These have been attributed to the breaking of C-C linkages between the lignin structural units (Ciobanu *et al.* 2004), as well as the fragmentation of inter-unit linkages (Gordobil *et al.* 2015). The temperature of this stage for LS was markedly lower than that of DLS, approximately in the range of 200 to 350 °C. This could be due to the release of water, CO_2 (Liu *et al.* 2008), CO, alkyls (Li *et al.* 2014), and possibly some SO_2. As a characteristic product of sulfonate compounds, the sulfonic acid groups pyrolyze at temperatures lower than 200 °C (Van Loon *et al.* 1993). The presence of SO_2 was indeterminable at this step. The third degradation step of LS occurred above 350 °C, with a substantial release of large molecular volatiles, aromatics, alkenes, and alkyls (Li *et al.* 2014). Additionally, the maximum weight loss rate in DLS was found to occur at 340 °C, while that of LS occurred at a lower temperature of 238 °C. Moreover, the levels of residue content at the end of the test for LS and DLS were found to be 62.72 ± 1.59% and 42.13 ± 2.73%, respectively. The higher char residue content of the LS has been attributed to higher sodium salts and chemically bonded sulfur (Leger *et al.* 2010).

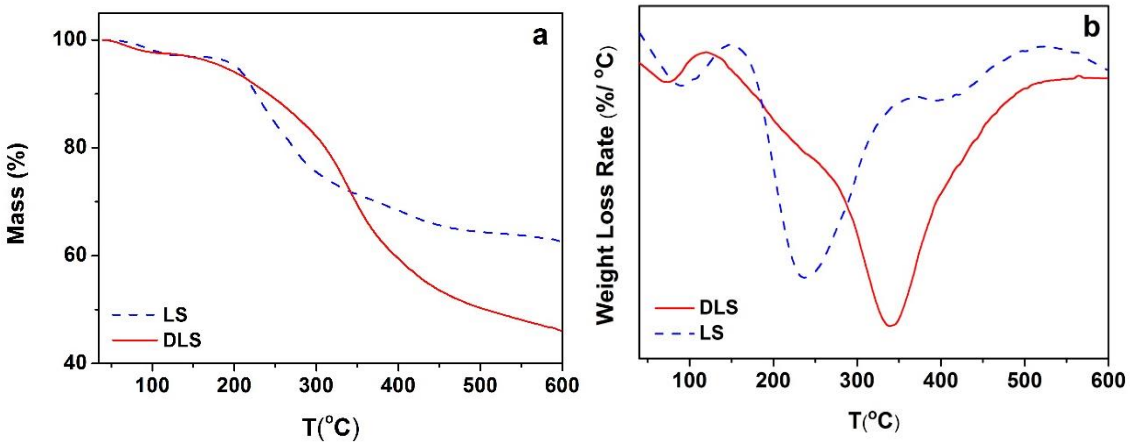

Fig. 3. (a) TG and (b) DTG curves of LS and DLS

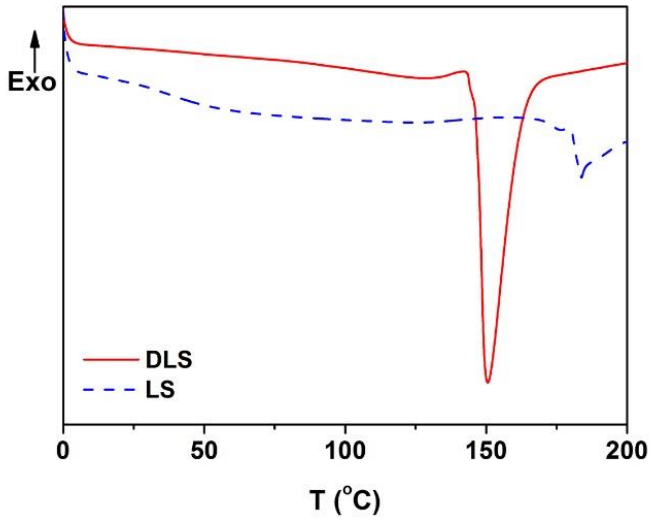

Fig. 4. DSC curves of LS and DLS

The DSC curves of LS and DLS are shown in Fig. 4. Due to the complex structure of lignin, the value of T_g was often difficult to measure. The T_g of lignins ranges from 90 to 180 °C in the literature (Li and McDonald 2014). In this study, it was remarkable that a sharp, strong exothermic melt peak was observed at 150 °C for DLS instead of the more typical glass transition at around 180 °C for LS. This could be associated with the lower molecular weight of DLS after desulfonation.

Properties of PLA/Lignin Composites

Thermal properties of PLA/lignin composites

Regarding the neat PLA and PLA composites with 5% and 10% LS and DLS, the (a) TG and (b) DTG curves are shown in Fig. 5, respectively. In addition, the onset degradation temperature ($T_{5\%}$), the maximum weight loss temperature (T_{max}), and the residue content are listed in Table 3.

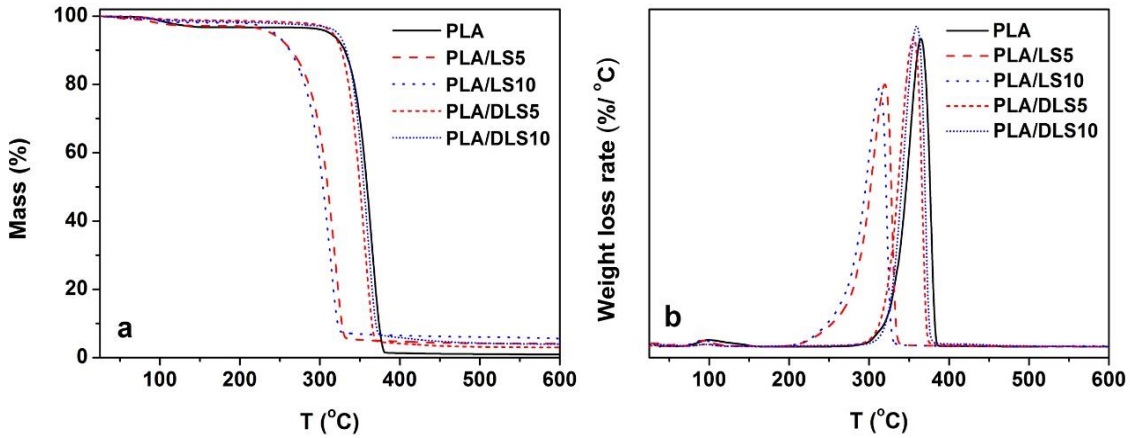

Fig. 5. (a) TG and (b) DTG curves of neat PLA and the composites

Table 3. Onset Degradation Temperature ($T_{5\%}$), Maximum Weight Loss Temperature (T_{max}), and Residue Content of Neat PLA and Composites

Sample Code	$T_{5\%}$ (°C)	T_{max} (°C)	Residue (%)
PLA	312	365	0.9
PLA/LS5	239	319	4.1
PLA/LS10	234	314	5.6
PLA/DLS5	316	356	2.9
PLA/DLS10	322	360	3.9

The thermal degradation of PLA involved a single degradation stage and was consistent with literature reports indicating that it occurs at 365 °C (Tran *et al.* 2014). The shapes of the overall TG and DTG curves of PLA/DLS were similar to those of the neat PLA. Composites including DLS displayed a slight increase in $T_{5\%}$ but a similar T_{max} compared with PLA. However, the inclusion of LS resulted in a dramatic decrease of the initial degradation and maximum decomposition temperatures compared with neat PLA and PLA/DLS composites. The higher thermal stability of PLA/DLS than that of PLA/LS was mostly due to the better thermal stability of DLS. Furthermore, the residue content increased as DLS and LS were added into the composites.

In addition, the thermal properties of the neat PLA and PLA/lignin composites were studied by DSC analysis (Fig. 6). The T_g increased in the PLA/DLS composites but remained almost unchanged in the PLA/LS composites. The increase in the T_g with the incorporation of DLS is an indication of the increased miscibility of this lignin with the PLA, whereas the LS appears to be immiscible since the T_g did not shift. Also, the endothermic peaks of samples at approximately 150 °C, associated with the melting point of PLA, were not considerably impacted by incorporating LS or DLS in PLA.

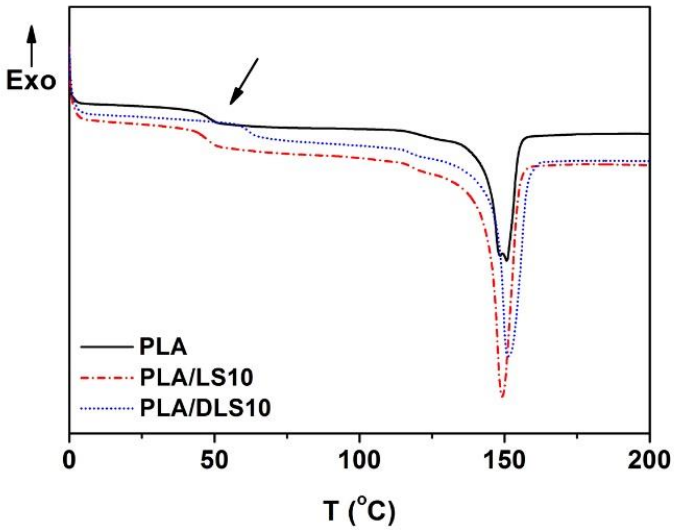

Fig. 6. DSC curves of neat PLA and PLA/lignin composites

Crystallization of PLA/lignin composites

X-ray diffraction patterns of the PLA and PLA/lignin composites are presented in Fig. 7. The XRD patterns of PLA reveal the typical diffraction peaks at 2θ = 14.76°,

16.7°, 19.1°, 22.4°, and 31.5°, which suggest that the layer distances of the PLA were 5.99, 5.31, 4.64, 3.96, and 2.84 nm, respectively.

The shape of the XRD pattern of the PLA/lignin composites was similar to that of neat PLA, indicating that there was no apparent change in crystallinity as a result of the introduction of the lignins as a nucleating agent. The same phenomenon has been observed with lignin in PHB (Weihua *et al.* 2004). The d_{200} and d_{203} peaks of PLA were noticeable in the PLA composites containing 10% LS and 5% DLS, which indicates that LS and DLS could accelerate the crystallization of PLA with an appropriately low content of lignin.

However, as the content of DLS became higher than 10%, all the peaks disappeared. Other researchers have detected a similar phenomenon where the polymer matrix was also reduced with increasing content of not only lignin, but also organoclay (Kubo and Kadla 2003; Gordobil *et al.* 2014). This has been found to act as a retardant if a strong interaction exists between the polymer matrix and the organoclay (Di *et al.* 2003; Lee *et al.* 2008). In a related research (Liao *et al.* 2007), it was found that a negligible amount of nucleating agent was present to help form the polymer crystal, whereas a higher nucleating agent content hindered the ordered arrangement of the molecular chain and resulted in low crystallinity.

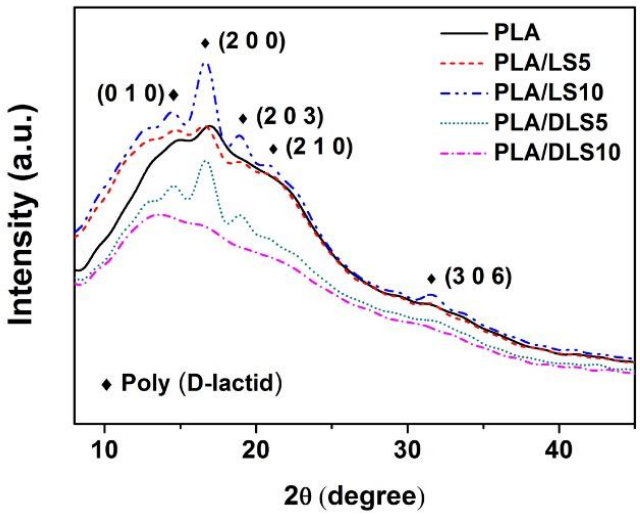

Fig. 7. X-ray diffraction patterns of the PLA and PLA/lignin composites

Moreover, in the cases when the lignin content was below 10%, crystallization was more prominent with the increase of LS, whereas the peaks became weaker with the increasing addition of DLS into the PLA matrix. Meanwhile, the size of the LS was much larger than that of the DLS, as illustrated in Fig. 8 (a) and (b). Such results appear to contradict, at least in part, previous observations that a filler using smaller particle sizes generally results in greater crystallinity (Tisserat *et al.* 2013). However, the diameter, shape, surface, and properties of nucleating agents affect the crystallinity of PLA (Liao *et al.* 2007). Therefore, the co-effects of size, content, and type of lignin particles acting as a nucleating agent should be taken into consideration.

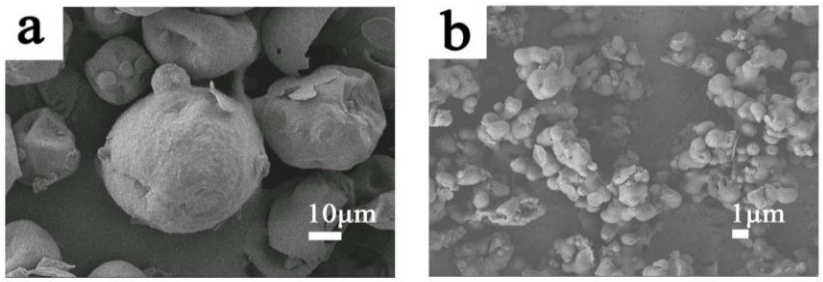

Fig. 8. SEM images of (a) LS and (b) DLS

Compatibility between PLA and lignin

The morphology of the lignin particles introduced into the PLA matrix is revealed in Fig. 9 to illustrate the compatibility between PLA and lignin. As evident in Fig. 8 (b), the size of the DLS particles (0.1 to 1 μm) became much smaller than that of the LS particles (10 to 30 μm) shown in Fig. 8 (a). Both LS and DLS have a large size distribution, due to the formation of inner molecular bonds with lignin molecules (Teixeira *et al.* 2012; Chen *et al.* 2014b). For the PLA/lignin composites, the homogeneous break surface of the neat PLA is shown in Fig. 9 (a). On the other hand, cavities of lignin particles in the modified PLA matrix were detected and are shown in Fig. 9 (b) and (c). The smaller size of lignin after desulfonation indicates the likelihood of greater compatibility with lignin within the PLA (Gordobil *et al.* 2014).

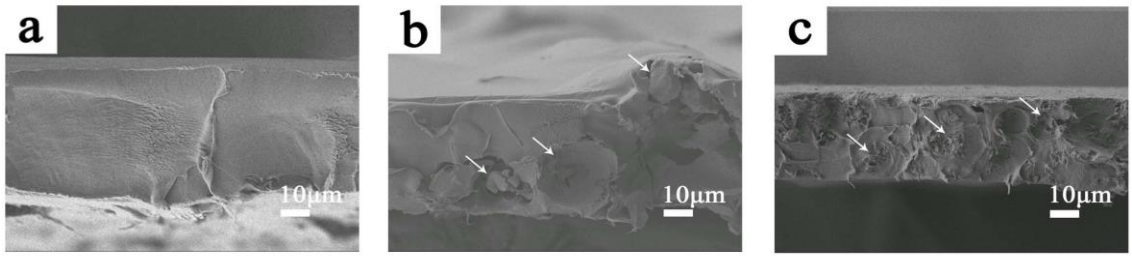

Fig. 9. SEM images of the break surface of PLA/lignin materials: (a) neat PLA, (b) PLA/LS5 and (c) PLA/DLS5

Contact angle of PLA/lignin composites

The contact angle was investigated to determine the hydrophobicity of PLA/lignin composites. The values of the contact angle of neat PLA and PLA/lignin composites are shown in Fig. 10. The contact angle of PLA/LS was lower than that of neat PLA and PLA/DLS. The hydrophilicity of the PLA/lignin composites was improved when a predetermined amount of LS was introduced into the PLA matrix, which is consistent with similar previously reported findings (Cazacu *et al.* 2016). However, the contact angle of PLA/DLS was higher than that of neat PLA and PLA/LS, and it increased with the growing content of DLS loadings. A better hydrophobicity was exhibited by the PLA/DLS composites, which was attributed to the lower contents of strong hydrophilic group ($-SO_3^-$) in DLS.

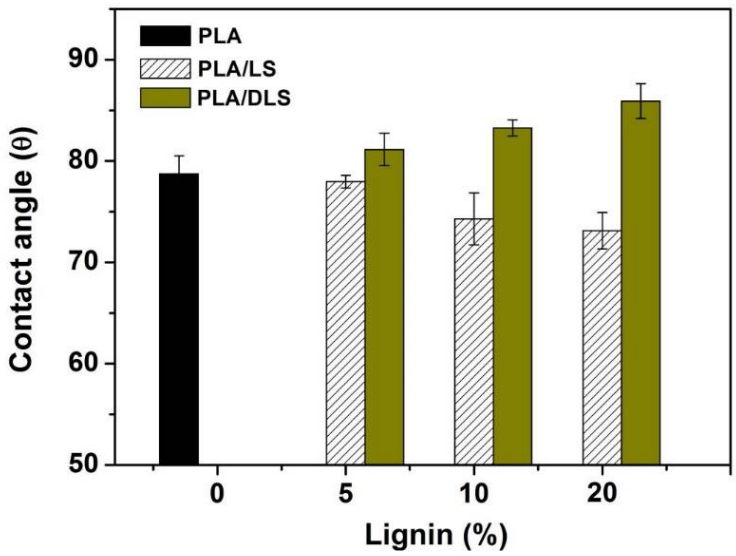

Fig. 10. Contact angle of neat PLA and PLA/lignin composites

Mechanical properties of PLA/lignin composites

Tensile tests were performed to study the effect of desulfonation on the mechanical properties of PLA/lignin composites. The tensile strength at break, elongation at break, and Young's modulus of the PLA composites with different percentages of LS or DLS are shown in Fig. 11.

The results reveal that PLA had better tensile strength compared with its composites, and this finding is in agreement with previously reported results for PLA/fiber composites (Razak *et al.* 2014). However, desulfonation mildly affected the mechanical properties of PLA/LS composites in all conditions by producing only a small decrease in maximum strength.

The slightly decreased mechanical strength in polymer/LS and PLA/lignin composites have also been reported by other researchers (Chung *et al.* 2013; Duval *et al.* 2013; Gordobil *et al.* 2015). In our case, the slight reduction in maximum strength resulted from irregular condensation and a random dispersion of tiny DLS spheres in the PLA matrix (Fig. 9).

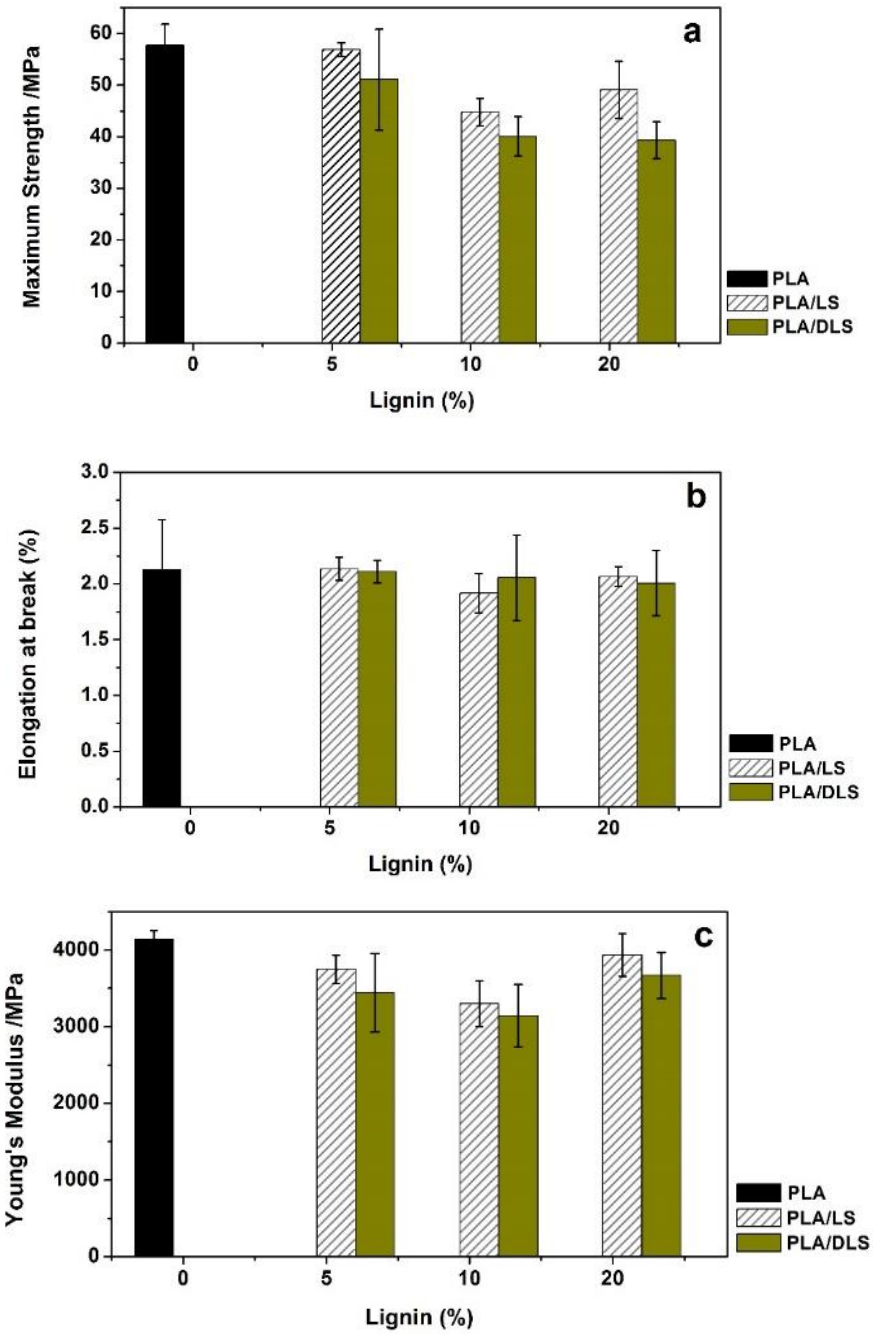

Fig. 11. Mechanical properties of neat PLA and PLA/lignin composites: effect of lignin content on (a) maximum tensile strength, (b) elongation at break, (c) Young's modulus of PLA, PLA/LS, and PLA/DLS composites

Optical properties of PLA/lignin composites

The absorption of UV light is a desirable property for plastic materials, helping to prevent damage and extend the shelf life of light-sensitive products (Ozdemir and Floros 2004; Agrawal *et al.* 2014; Heinrich *et al.* 2015; Lizundia *et al.* 2016). PLA/lignin

composites and pure PLA were used to investigate UV light absorption by UV-Vis measurement.

The optical absorption spectra within the UV region (190 to 400 nm) for the specimens are shown in Fig. 12. It is important to mention that absorbance of UV light occurred at approximately 220 to 250 nm in all PLA/lignin specimens, and the UV absorbance increased as lignin was introduced into the PLA matrix. Both PLA/LS and PLA/DLS could potentially be applied to help protect light-sensitive products from UV light damage.

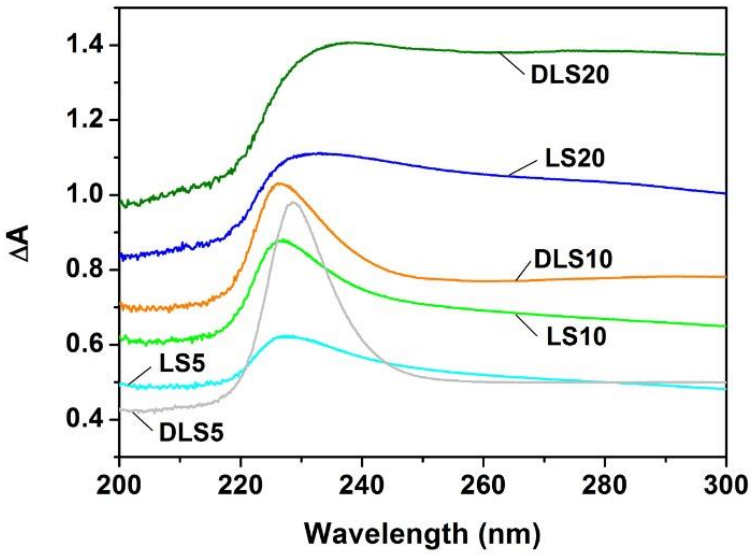

Fig. 12. UV−Vis absorbance spectra of PLA/lignin composites

CONCLUSIONS

1. In this study, the basic structure of lignin remained after desulfonation. A marked decrease in the M_w (For LS, M_w = 2329 g·mol^{-1}; for DLS, M_w = 635 g·mol^{-1}) and sulfur content (DLS = 2.32 ± 0.11%, LS = 5.78 ± 0.58%) of LS was caused by desulfonation. Moreover, the maximum weight loss rate upon heating of DLS was much lower, which showed an improved thermal stability after desulfonation. Additionally, the high char residue contents of LS and DLS were found to be 62.72 ± 1.59% and 42.13 ± 2.73%, respectively.
2. In addition, the PLA/lignin composites were successfully fabricated by the casting method. The enhanced hydrophobicity of PLA/DLS composites after desulfonation was measured through contact angle. The results revealed that PLA/DLS had a better thermal stability (T_{max} = 360 °C) than PLA/LS (T_{max} = 314 °C). Meanwhile, the T_g increased in PLA/DLS but was unchanged in PLA/LS composites. Also, the endothermic peaks of PLA/lignin composites, associated with the melting point of PLA, were not considerably impacted by incorporating LS or DLS in the PLA matrix.

Moreover, both LS and DLS acted as nucleating agents at low content (5% for PLA/DLS and 10% for PLA/LS) in PLA. A greater compatibility between PLA and DLS was detected as a result of the smaller size of lignin (0.1 to 1 μm) obtained after desulfonation. However, the effect of desulfonation of LS was quite small with respect to UV absorption and the mechanical properties of PLA/lignin specimens. A strong UV absorption at 220 to 250 nm and almost unchanged mechanical properties were detected in both PLA/LS and PLA/DLS composites.

ACKNOWLEDGMENTS

The authors are grateful for the financial support from the Co-built Project Beijing Municipal Education Commission (2016) "R & D on Technology in Scientific Utilization of Non-Wood Plant Material".

REFERENCES CITED

Afrin, T., Tsuzuki, T., and Wang, X. (2012). "UV absorption property of bamboo," *Journal of the Textile Institute* 103(4), 394-399. DOI: 10.1080/00405000.2011.580543

Agrawal, A., Kaushik, N., and Biswas, S. (2014). "Derivatives and applications of lignin-An insight," *The SciTech Journal* 1(7), 30-36.

Alay, E., Duran, K., and Korlu, A. (2016). "A sample work on green manufacturing in textile industry," *Sustainable Chemistry and Pharmacy* 3, 39-46. DOI: 10.1016/j.scp.2016.03.001

ASTM D3246-15 (2015). "Standard test method for sulfur in petroleum gas by oxidative microcoulometry," ASTM International, West Conshohocken, PA.

Bozsódi, B., Romhányi, V., Pataki, P., Kun, D., Renner, K., and Pukánszky, B. (2016). "Modification of interactions in polypropylene/lignosulfonate blends," *Materials and Design* 103, 32-39. DOI: 10.1016/j.matdes.2016.04.061

Brizius, G. L., and Montgomery, P. K. (2014). "Tailorable lignosulfonate carbonate adhesives," Patent No. US 8864892 B2.

Cazacu, G., Darie-Nita, R. N., Chirila, O, Totolin, M., Asandules, M., Ciolacu, D. E., Ludwiczak, J., and Vasile, C. (2016). "Environmentally friendly polylactic acid/modified lignosulfonate biocomposites," *Journal of Polymers and the Environment* 1-19. DOI: 10.1007/s10924-016-0868-2

Chen, G., Zhang, J., Yang, N. W., and Ma, Y. F. (2014a). "The evaluation of sodium hydroxymethyl lignosulfonate as an ecofriendly drilling fluid additive," *Petroleum Science and Technology* 32(15), 1816-1823. DOI: 10.1080/10916466.2011.642916

Chen, R., Abdelwahab, M. A., Misra, M., and Mohanty, A.K. (2014b). "Biobased ternary blends of lignin, poly (lactic acid), and poly (butylene adipate-co-terephthalate): The effect of lignin heterogeneity on blend morphology and compatibility," *Journal of Polymers and the Environment* 22(4), 439-448. DOI: 10.1007/s10924-014-0704-5

Chung, Y.-L., Olsson, J. V., Li, R. J., Frank, C. W., Waymouth, R. M., Billington, S. L., and Sattely, E. S. (2013). "A renewable lignin-lactide copolymer and application in biobased composites," *ACS Sustainable Chemistry and Engineering* 1(10), 1231-1238. DOI: 10.1021/sc4000835

Ciobanu, C., Ungureanu, M., Ignat, L., Ungureanu, D., and Popa, V. (2004). "Properties of lignin-polyurethane films prepared by casting method," *Industrial Crops and Products* 20(2), 231-241. DOI: 10.1016/j.indcrop.2004.04.024

DeBons, F. E., Pedersen, L. D., and Whittington, L. E. (1992). "Use of lignin/amine/surfactant blends in enhanced oil recovery." U.S. Patent No. 5114599.

Di, Y., Iannace, S., Di Maio, E., and Nicolais, L. (2003). "Nanocomposites by melt intercalation based on polycaprolactone and organoclay," *Journal of Polymer Science Part B: Polymer Physics* 41(7), 670-678. DOI: 10.1002/polb.10420

Domenek, S., Louaifi, A., Guinault, A., and Baumberger, S. (2013). "Potential of lignins as antioxidant additive in active biodegradable packaging materials," *Journal of Polymers and the Environment* 21(3), 692-701. DOI: 10.1007/s10924-013-0570-6

Duval, A., Molina-Boisseau, S., and Chirat, C. (2013). "Comparison of kraft lignin and lignosulfonates addition to wheat gluten-based materials: Mechanical and thermal properties," *Industrial Crops and Products* 49, 66-74. DOI: 10.1016/j.indcrop.2013.04.027

El Hage, R., Brosse, N., Chrusciel, L., Sanchez, C., Sannigrahi, P., and Ragauskas, A. (2009). "Characterization of milled wood lignin and ethanol organosolv lignin from miscanthus," *Polymer Degradation and Stability* 94(10), 1632-1638. DOI: 10.1016/j.polymdegradstab.2009.07.007

El Mansouri, N., and Salvadó, J. (2006). "Structural characterization of technical lignins for the production of adhesives: Application to lignosulfonate, kraft, soda-anthraquinone, organosolv, and ethanol process lignins," *Industrial Crops and Products* 24(1), 8-16. DOI: 10.1016/j.indcrop.2005.10.002

Ferry, L., Dorez, G., Taguet, A., Otazaghine, B., and Lopez-Cuesta, J. (2015). "Chemical modification of lignin by phosphorus molecules to improve the fire behavior of polybutylene succinate," *Polymer Degradation and Stability* 113, 135-143. DOI: 10.1016/j.polymdegradstab.2014.12.015

Fischer, K., and Schiene, R. (2002). "Nitrogenous fertilizers from lignins—A review," in: *Chemical Modification, Properties, and Usage of Lignin*, Thomas Q. Hu (ed.), Springer US, New York, NY, pp. 167-198.

Gordobil, O., Egüés, I., Llano-Ponte, R., and Labidi, J. (2014). "Physicochemical properties of PLA lignin blends," *Polymer Degradation and Stability* 108, 330-338. DOI: 10.1016/j.polymdegradstab.2014.01.002

Gordobil, O., Delucis, R., Egüés, and I., Labidi, J. (2015). "Kraft lignin as filler in PLA to improve ductility and thermal properties," *Industrial Crops and Products* 72, 46-53. DOI: 10.1016/j.indcrop.2015.01.055

Hatakeyama, H., Matsumura, H., and Hatakeyama, T. (2013). "Glass transition and thermal degradation of rigid polyurethane foams derived from castor oil–molasses polyols," *Journal of Thermal Analysis and Calorimetry* 111(2), 1545-1552. DOI: 10.1007/s10973-012-2501-5

Heinrich, V., Zunabovic, M., Bergmair, J., Kneifel, W., and Jäger, H. (2015). "Post-packaging application of pulsed light for microbial decontamination of solid foods: A review," *Innovative Food Science and Emerging Technologies* 30, 145-156. DOI: 10.1016/j.ifset.2015.06.005

Hu, J., and Guo, M. (2015). "Influence of ammonium lignosulfonate on the mechanical and dimensional properties of wood fiber biocomposites reinforced with polylactic acid," *Industrial Crops and Products* 78, 48-57. DOI: 10.1016/j.indcrop.2015.09.075

Imre, B., Bedő, D., Domján, A., Schön, P., Vancso, G. J., and Pukánszky, B. (2013). "Structure, properties and interfacial interactions in poly (lactic acid)/polyurethane blends prepared by reactive processing," *European Polymer Journal* 49(10), 3104-3113. DOI: 10.1016/j.eurpolymj.2013.07.007

Indraratna, B., Athukorala, R., and Vinod, J. (2012). "Estimating the rate of erosion of a silty sand treated with lignosulfonate," *Journal of Geotechnical and Geoenvironmental Engineering* 139(5), 701-714. DOI: 10.1061/(ASCE)GT.1943-5606.0000766

Keshk, S., and Sameshima, K. (2006). "Influence of lignosulfonate on crystal structure and productivity of bacterial cellulose in a static culture," *Enzyme and Microbial Technology* 40(1), 4-8. DOI: 10.1016/j.enzmictec.2006.07.037

Kim, H., Na, H. Y., Lee, J. H., and Lee, S. J. (2015). "Preparation, morphology and electrical conductivity of polystyrene/polydopamine-carbon nanotube microcellular foams via high internal phase emulsion polymerization," *Polymer Korea* 39(2), 293-299. DOI: 10.7317/pk.2015.39.2.293

Komissarenkov, A., and Lukanina, T. (2012). "Use of lignosulfonates in newsprint paper production," *Russian Journal of General Chemistry* 82(5), 985-990. DOI: 10.1134/S1070363212050325

Kubo, S., and Kadla, J. F. (2003). "The formation of strong intermolecular interactions in immiscible blends of poly (vinyl alcohol)(PVA) and lignin," *Biomacromolecules* 4(3), 561-567. DOI: 10.1021/bm025727p

Lee, S. Y., Chen, H., and Hanna, M. A. (2008). "Preparation and characterization of tapioca starch-poly(lactic acid) nanocomposite foams by melt intercalation based on clay type," *Industrial Crops and Products* 28(1), 95-106. DOI: 10.1016/j.indcrop.2008.01.009

Leger, C. A., Chan, F. D., and Schneider, M. H. (2010). "Fractionation and characterisation of technical ammonium lignosulphonate," *BioResources* 5(4), 2239-2247. DOI: 10.15376/biores.5.4.2239-2247

Li, X. (2011). "Preparation and properties of biodegradable sodium lignosulfonate/poly (vinyl alcohol) blend films," *Advanced Materials Research* 160-162, 676-681. DOI: 10.4028/www.scientific.net/AMR.160-162.676

Li, H., and McDonald, A. G. (2014). "Fractionation and characterization of industrial lignins," *Industrial Crops and Products* 62, 67-76. DOI: 10.1016/j.indcrop.2014.08.013

Li, B., Lv, W., Zhang, Q., Wang, T., and Ma, L. (2014). "Pyrolysis and catalytic pyrolysis of industrial lignins by TG-FTIR: Kinetics and products," *Journal of Analytical and Applied Pyrolysis* 108, 295-300. DOI: 10.1016/j.jaap.2014.04.002

Liang, F. B., Song, Y. L., Huang, C. P., Zhang, J., and Chen, B. H. (2013). "Adsorption of hexavalent chromium on a lignin-based resin: Equilibrium, thermodynamics, and kinetics," *Journal of Environmental Chemical Engineering* 1(4), 1301-1308. DOI: 10.1016/j.jece.2013.09.025

Liao, R., Yang, B., Yu, W., and Zhou, C. (2007). "Isothermal cold crystallization kinetics of polylactide/nucleating agents," *Journal of Applied Polymer Science* 104(1), 310-317. DOI: 10.1002/app.25733

Lin, N., Fan, D., Chang, P. R., Yu, J., Cheng, X., and Huang, J. (2011). "Structure and properties of poly(butylene succinate) filled with lignin: A case of lignosulfonate," *Journal of Applied Polymer Science* 121(3), 1717-1724. DOI: 10.1002/app.33754

Lisperguer, J., Perez, P., and Urizar, S. (2009). "Structure and thermal properties of lignins: Characterization by infrared spectroscopy and differential scanning calorimetry," *Journal of the Chilean Chemical Society* 54(4), 460-463. DOI: 10.4067/S0717-97072009000400030

Liu, Q., Wang, S., Zheng, Y., Luo, Z., and Cen, K. (2008). "Mechanism study of wood lignin pyrolysis by using TG-FTIR analysis," *Journal of Analytical and Applied Pyrolysis* 82(1), 170-177. DOI: 10.1016/j.jaap.2008.03.007

Liu, R., Peng, Y., and Cao, J. (2016). "Thermal stability of organo-montmorillonite-modified wood flour/poly (lactic acid) composites," *Polymer Composites* 37(7), 1971-1977. DOI: 10.1002/pc.23375

Lizundia, E., Ruiz-Rubio, L., Vilas, J. L., and León, L. M. (2016). "Poly(l-lactide)/ZnO nanocomposites as efficient UV-shielding coatings for packaging applications," *Journal of Applied Polymer Science* 132, 42426. DOI: 10.1002/app.42426

Lummer, N. R., and Plank, J. (2012). "Combination of lignosulfonate and AMPS®-co-NNDMA water retention agent – An example for dual synergistic interaction between admixtures in cement," *Cement and Concrete Research* 42(5), 728-735. DOI: 10.1016/j.cemconres.2012.02.009

Núñez-Flores, R., Giménez, B., Fernández-Martín, F., López-Caballero, M., Montero, M., and Gómez-Guillén, M. (2012). "Role of lignosulphonate in properties of fish gelatin films," *Food Hydrocolloids* 27(1), 60-71. DOI: 10.1016/j.foodhyd.2011.08.015

Ozdemir, M., and Floros, J. D. (2004). "Active food packaging technologies," *Critical Reviews in Food Science and Nutrition* 44(3), 185-193. DOI: 10.1080/10408690490441578

Pan, Y., Zhan, J., Pan, H., Wang, W., Tang, G., Song, L., and Hu, Y. (2016). "Effect of fully biobased coatings constructed via layer-by-layer assembly of chitosan and lignosulfonate on the thermal, flame retardant, and mechanical properties of flexible polyurethane foam," *ACS Sustainable Chemistry and Engineering* 4(3), 1431-1438. DOI: 10.1021/acssuschemeng.5b01423

Pang, B., Yan, J., Yao, L., Liu, H., Guan, J., Wang, H., and Liu, H. (2016). "Preparation and characterization of antibacterial paper coated with sodium lignosulfonate stabilized ZnO nanoparticles," *RSC Advances* 6(12), 9753-9759. DOI: 10.1039/C5RA21434C

Pye, E. K. (2008). "Industrial lignin production and applications," in: *Biorefineries-Industrial Processes and Products: Status Quo and Future Directions*, B. Kamm, P.

R. Gruber, and M. Kamm (eds.), Wiley-VCH, Weinheim, Germany, pp. 165-200. DOI: 10.1002/9783527619849.ch22

Razak, N. I. A., Ibrahim, N. A., Zainuddin, N., Rayung, M., and Saad, W. Z. (2014). "The influence of chemical surface modification of kenaf fiber using hydrogen peroxide on the mechanical properties of biodegradable kenaf fiber/poly(lactic acid) composites," *Molecules* 19(3), 2957-2968. DOI: 10.3390/molecules19032957

Revin, V. V., Novokuptsev, N. V., and Kadimaliev, D. A. (2016). "Preparation of biocomposites using sawdust and lignosulfonate with a culture liquid of levan producer azotobacter vinelandii as a bonding agent," *BioResources* 11(2), 3244-3258. DOI: 10.15376/biores.11.2.3244-3258

Saito, T., Perkins, J. H., Vautard, F., Meyer, H. M., Messman, J. M., Tolnai, B., and Naskar, A. K. (2014). "Methanol fractionation of softwood kraft lignin: Impact on the lignin properties," *ChemSusChem* 7(1), 221-228. DOI: 10.1002/cssc.201300509

Sallem-Idrissi, N., Vanderghem, C., Pacary, T., Richel, A., Debecker, D. P., Devaux, J., and Sclavons, M. (2016). "Lignin degradation and stability: Volatile organic compounds (VOCs) analysis throughout processing," *Polymer Degradation and Stability* 130, 30-37. DOI: 10.1016/j.polymdegradstab.2016.05.028

Scholze, B., Hanser, C., and Meier, D. (2001). "Characterization of the water-insoluble fraction from fast pyrolysis liquids (pyrolytic lignin): Part II. GPC, carbonyl goups, and 13C-NMR," *Journal of Analytical and Applied Pyrolysis* 58-59, 387-400. DOI: 10.1016/S0165-2370(00)00173-X

Shankar, S., Reddy, J. P., and Rhim, J. W. (2015). "Effect of lignin on water vapor barrier, mechanical, and structural properties of agar/lignin composite films," *International Journal of Biological Macromolecules* 81, 267-273. DOI: 10.1016/j.ijbiomac.2015.08.015

Strassberger, Z., Prinsen, P., van der Klis, F., van Es, D. S., Tanase, S., and Rothenberg, G. (2015). "Lignin solubilisation and gentle fractionation in liquid ammonia," *Green Chemistry* 17(1), 325-334. DOI: 10.1039/c4gc01143k

Suganuma, S., Nakajima, K., Kitano, M., Yamaguchi, D., Kato, H., and Hayashi, S. (2008). "Hydrolysis of cellulose by amorphous carbon bearing SO_3H, COOH, and OH groups," *Journal of the American Chemical Society* 130(38), 12787-12793. DOI: 10.1021/ja803983h

Surendra, K., Sawatdeenarunat, C., Shrestha, S., Sung, S., and Khanal, S. K. (2015). "Anaerobic digestion-based biorefinery for bioenergy and biobased products," *Industrial Biotechnology* 11(2), 103-112. DOI: 10.1089/ind.2015.0001

Teixeira, E. D. M., Curvelo, A. A., Corrêa, A. C., Marconcini, J. M., Glenn, G. M., and Mattoso, L. H. (2012). "Properties of thermoplastic starch from cassava bagasse and cassava starch and their blends with poly (lactic acid)," *Industrial Crops and Products* 37(1), 61-68. DOI: 10.1016/j.indcrop.2011.11.036

Thakur, V. K., and Thakur, M. K. (2015). "Recent advances in green hydrogels from lignin: A review," *International Journal of Biological Macromolecules* 72, 834-847. DOI: 10.1016/j.ijbiomac.2014.09.044

Tisserat, B., Joshee, N., Mahapatra, A. K., Selling, G. W., and Finkenstadt, V. L. (2013). "Physical and mechanical properties of extruded poly (lactic acid)-based *Paulownia*

elongata biocomposites," *Industrial Crops and Products* 44, 88-96. DOI: 10.1016/j.indcrop.2012.10.030

Tran, T. P. T., Bénézet, J. C., and Bergeret, A. (2014). "Rice and einkorn wheat husks reinforced poly(lactic acid) (PLA) biocomposites: Effects of alkaline and silane surface treatments of husks," *Industrial Crops and Products* 58, 111-124. DOI: 10.1016/j.indcrop.2014.04.012

Van Loon, W. M., Boon, J. J., and de Groot, B. (1993). "Quantitative analysis of sulfonic acid groups in macromolecular lignosulfonic acids and aquatic humic substances by temperature-resolved pyrolysis-mass spectrometry," *Environmental Science and Technology* 27(12), 2387-2396. DOI: 10.1021/es00048a012

Weihua, K., He, Y., Asakawa, N., and Inoue, Y. (2004). "Effect of lignin particles as a nucleating agent on crystallization of poly(3-hydroxybutyrate)," *Journal of Applied Polymer Science* 94(6), 2466-2474. DOI: 10.1002/app.21204

Yang, D., Chang, Y., Wu, X., Qiu, X., and Lou, H. (2014). "Modification of sulfomethylated alkali lignin catalyzed by horseradish peroxidase," *RSC Advances* 4(96), 53855-53863. DOI: 10.1039/C4RA07244H

Yang, W., Dominici, F., Fortunati, E., Kenny, J., and Puglia, D. (2015). "Effect of lignin nanoparticles and masterbatch procedures on the final properties of glycidyl methacrylate-*g*-poly (lactic acid) films before and after accelerated UV weathering," *Industrial Crops and Products* 77, 833-844. DOI: 10.1016/j.indcrop.2015.09.057

Ye, D. Z., Jiang, L., Hu, X. Q., Zhang, M. H., and Zhang, X. (2016). "Lignosulfonate as reinforcement in polyvinyl alcohol film: Mechanical properties and interaction analysis," *International Journal of Biological Macromolecules* 83, 209-215. DOI: 10.1016/j.ijbiomac.2015.11.064

Yu, Y., Fu, S., Song, P.a., Luo, X., Jin, Y., Lu, F., Wu, Q., and Ye, J. (2012). "Functionalized lignin by grafting phosphorus-nitrogen improves the thermal stability and flame retardancy of polypropylene," *Polymer Degradation and Stability* 97, 541-546. DOI: 10.1016/j.polymdegradstab.2012.01.020

Zafar, S., Ahmed, R., and Khan, R. (2016). "Biotransformation: A green and efficient way of antioxidant synthesis," *Free Radical Research* 50(9), 939-948. DOI: 10.1080/10715762.2016.1209745

Zhou, G., Taylor G., and Polle, A. (2011). "FTIR-ATR-based prediction and modelling of lignin and energy contents reveals independent intra-specific variation of these traits in bioenergy poplar," *Plant Methods 7(9).* DOI: 10.1186/1746-4811-7-9

Article submitted: February 23, 2017; Peer review completed: April 6, 2017; Revised version received and accepted: May 5, 2017; Published: May 16, 2017.
DOI: 10.15376/biores.12.3.4810-4829